Journal Pre-proof

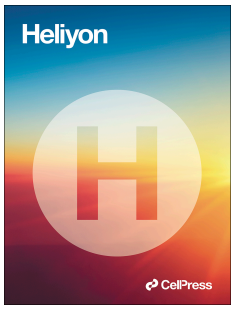

3D-printed zeolite 13X-Strontium chloride units as ammonia carriers

Nasir Shezad, Marco D'Agostini, Ali Ezzine, Giorgia Franchin, Paolo Colombo, Farid Akhtar

PII: S2405-8440(23)06584-2

DOI: https://doi.org/10.1016/j.heliyon.2023.e19376

Reference: HLY 19376

To appear in: *HELIYON*

Received Date: 4 April 2023

Revised Date: 21 August 2023

Accepted Date: 21 August 2023

Please cite this article as: , 3D-printed zeolite 13X-Strontium chloride units as ammonia carriers, *HELIYON* (2023), doi: https://doi.org/10.1016/j.heliyon.2023.e19376.

Author Contributions

Nasir Shezad: Methodology, characterizations, sorption measurements, formal analysis, kinetics, writing the original draft preparation.

Marco D'Agostini: Methodology, characterizations, formal analysis and original draft preparation.

Ali Ezzine: Methodology and characterizations

Giorgia Franchin: Supervision, funding, and reviewing, correcting the original draft.

Paolo Colombo: Supervision and funding

Farid Akhtar: Conceptualization, design, methodology, supervision, funding, writing, reviewing, and correcting the original draft.

3D-Printed Zeolite 13X-Strontium Chloride Units as Ammonia Carriers

Nasir Shezad[a], Marco D'Agostini[b], Ali Ezzine[b], Giorgia Franchin[b], Paolo Colombo[b], Farid Akhtar[a*]

[a]Division of Materials Science, Department of Engineering Sciences and Mathematics, Luleå University of Technology, Luleå SE-971 87, Sweden

[b]Department of Industrial Engineering, University of Padova, Via Marzolo, 9, Padova, 35131, Italy

*Corresponding author: farid.akhtar@ltu.se

Abstract:

The selctive catalytic reduction (SCR) system in automobile using urea solution as a source of NH_3 suffer from solid deposit problem in pipe lines and poor efficiency during engine startup. Although direct use of high pressure NH_3 is restricted due to safety concern, which can be overcome by using solid sorbents as NH_3 carrier. Strontium chloride ($SrCl_2$) is considered the best sorbent due to its high sorption capacity; however, challenges are associated with the processing of stable engineering structures due to extraordinary volume expansion during the NH_3 sorption. This study reports the fabrication of a novel structure consisting of a zeolite cage enclosing the $SrCl_2$ pellet (SPZC) through extrusion-based 3D printing (Direct Ink Writing). The printed SPZC structure demonstrated steady sorption of NH_3 for 10 consecutive cycles without significant uptake capacity and structural integrity loss. Furthermore, the structure exhibited improved sorption and desorption kinetics than pure $SrCl_2$. The synergistic effect of zeolite as physisorbent and $SrCl_2$ as chemisorbent in the novel composite structure enabled the low-pressure (< 0.4 bar) and high-pressure (> 0.4 bar) NH_3 sorption, compared to pure $SrCl_2$, which absorbed NH_3 at pressures above 0.4 bar. Regeneration of SPZC composite sorbent under evacuation showed that 87.5% percent of NH_3 was desorbed at 20 ^oC. Thus, the results demonstrate that the rationally designed novel SPZC structure offers safe and efficient storage of NH_3 in the SCR system and other applications.

Keywords: 3D printed structure, Ammonia, Zeolite, Alkaline earth metal halides, Physicochemical sorption, Kinetics.

1 Introduction:

The combustion of fossil fuels releases various pollutants into the air, such as sulphur oxide (SOx), nitrogen oxide (NOx), and carbon oxide (COx). The mortalities during the COVID-19 pandemic have shown the link between pollution, especially NOx and particulate matter, and the coronavirus's mortality rate [1][2]. The major sources of NOx emission are fossil fuel power plants and the transport sector. A selective catalytic reduction system in the transport sector converts NOx into elemental N_2 and water. Usually, this method uses urea solution to generate NH_3, which acts as a reductant to reduce NOx into harmless compounds. The efficiency of the technique is quite good (around 95%), and it is successfully applied for commercial applications [3][4]. However, the urea solution cannot operate below -11 ^oC and freezes, which could damage the diesel exhaust fluid (DEF) filled tank. In addition, the process involves the hydrolysis of urea to produce NH_3, which is slow during engine startup time due to lower temperatures in the SCR system. Thus, there is a delay in the supply of NH_3 in the SCR reaction, which may let some NOx into the environment and may lead to deposit formation in the pipe lines [5]. The problem can be overcome by using solid NH_3 carriers that supply NH_3 without delay and can work at low temperatures without solid deposit formation [6][7]. These NH_3 sorbent unit would be easy to replaced or recharged depending upon the type of sorbent material Also, the sorbent-based SCR system would be compact and lightweight compared to typical urea-based systems [8].

Due to their high capacity, alkaline earth metal halides (AEMHs) have been used for NH_3 sorption. The sorption of NH_3 over AEMHs proceeds through forming a metal ammine complex. Among AEMHs, $SrCl_2$ has the highest NH_3 uptake as it forms an amine complex with 8 molecules of NH_3, for instance, compared to $MgCl_2$, which forms an amine complex with 6 molecules of NH_3 [7]. Further, the binding energies of NH_3 molecules with $MgCl_2$ are higher than $SrCl_2$, and a high temperature is needed for regeneration [8][9][10]. During the ammonia sorption, AEMHs undergo expansion in volume, ca. 400% for $MgCl_2$ and ca.300% for $SrCl_2$ [11][12]. Therefore, most structured AEMHs adsorbents are unstable during ammonia sorption and disintegrate into powder. The powder formation can increase the pressure drop across the bed, which is detrimental to the adsorption system as it could damage the reaction chamber [13]. Additionally, the metal-amine complex formation occurs when NH_3 gives its lone pair electrons to metal ions of AEMHs, thereby releasing exothermic heat of reaction which affects the thermal stability and, subsequently, the structural integrity of the sorbent. Thus, these challenges are the hurdle in fabricating stable and robust structures of the AEMHs.

Another challenge is the sluggish sorption kinetics of $SrCl_2$ and low adsorption capacity at low pressure (below 0.4 bar) at normal conditions [12][14][7][8]. Recently, Cao et al. reported the structured $SrCl_2$, $SrCl_2$/graphite, $SrCl_2$/rGO, and MOF composites using the freeze-casting method. Those composites showed good efficiency concerning NH_3 uptake and sorption kinetics [12], [14], [15]. However, extraordinary volume changes are expected during NH_3 sorption for typical structures and composites of AEMHs. Besides, freeze casting is a tedious and comparatively less efficient approach with the limited choice of solvent and to fabricate complex structures such as monoliths [16]. On the other hand, 3D printing is a modern approach to fabricating complex and highly efficient structures for various applications. The advantage of 3D printing technique is accuracy, smoothness of the structure, low waste material, and complex geometries [17]. Moreover, unlike freeze casting, in 3D printing, various types of complex structures can be designed and printed without special molds.

This study focuses on devising a concept of structured cages for $SrCl_2$ to accommodate volume swings associated with NH_3 sorption. These cages could provide the necessary free space for the volume expansion of the $SrCl_2$ during the formation of the amine complex and act as a barrier for spreading powder. The capacity of $SrCl_2$ remains intact, and it can absorb the same amount of NH_3 as that of powder. Therefore, the disintegration of the $SrCl_2$ unit inside the cage would not create structural or functional problems until it remained enclosed. Further, the selection of material for the cage is crucial. A good sorbent material like zeolite can be the best choice owing to its availability, stability, and ability to capture the NH_3. Interestingly, zeolites adsorb NH_3 at lower pressure, significantly below the working pressure of the $SrCl_2$. Furthermore, zeolites capture the NH_3 through physical adsorption rather than chemisorption [18]–[21]. Therefore, combining zeolite and $SrCl_2$ can improve the NH_3 uptake and solve the problem of poor adsorption activity of $SrCl_2$ at low-pressure conditions. In this work, we 3D printed a zeolite 13X cage enclosing $SrCl_2$ pellet inside (SPZC) using a Direct Ink Writing technique. The sorbents were characterized using X-ray diffraction(XRD), nitrogen adsorption and desorption, scanning electron microscopy (SEM), and thermogravimetric analysis (TGA) technique. The sorbent demonstrated excellent NH_3 uptake for 10 consecutive cycles without formation of loose particles or powder inside the sorption chamber. The kinetic data has shown that adding zeolite enhances the NH_3 sorption at low-pressure regions.

2 Material and methods:

2.1 Fabrication of pellets and Zeolite cage:

Zeolite 13X cages of cylindrical design (Ø10 x 5 mm) to contain the $SrCl_2$ pellets during NH_3 sorption were 3D printed by Direct Ink Writing. A schematic of the process is illustrated in Fig. 1. A potassium geopolymer with the molar composition of 3.8 SiO_2 – Al_2O_3 – K_2O synthesized from metakaolin (Argical 1200S, Imerys, France) and an alkaline solution of potassium silicate (Kasolv 205, PQ Corporation, The Netherlands), potassium hydroxide (Honeywell Research Chemicals, USA) and distilled water were chosen as the structural matrix for the zeolite particles. The alkaline solution was prepared in advance and aged for 12 h at 40 °C to allow for a complete dissolution of the reagents.

The slurry for Direct Ink Writing was prepared in an ice bath by adding the metakaolin and fillers to the alkaline solution under high-shear mechanical mixing. The temperature of the slurry was maintained close to 0 °C at all times to delay the onset of geopolymer polycondensation, which would have resulted in a rapid loss of workability. The composition of the solid fraction of the slurry, on a dry basis, is 60 wt.% zeolite 13X (2-4 μm, Luoyang Jianlong Chemical Industry Co., Ltd), 3 wt.% Na-bentonite (ClearOFF Minerals, UK) as a rheological additive, 2 wt.% carboxymethylcellulose (Sigma, Germany) as a stabilizing agent and 35 wt.% K-geopolymer; good printability was achieved with a solid-to-liquid ratio of 1.93 by weight. After 30 minutes of mixing, the slurry was transferred to a syringe (Vieweg, Germany) and defoamed on a high-energy planetary mixer (ARE-250, Thinky Corporation, Japan).

3D printing of the cages was carried out on a Direct Ink Writing printer (Delta WASP 2040 Turbo, WASP, Italy) equipped with an Auger screw extruder (LDM Extruder 3.0, WASP, Italy) and a 580 μm tapered nozzle (Vieweg, Germany). The syringe, refrigerated using a cooling jacket, acts as a reservoir from which the slurry is pushed into the extruder chamber by compressed air and finally deposited onto the build plate. After printing, the samples were cured for 7 days at room temperature and ≈100% R.H., then dried at 75 °C overnight and heat-treated at 450 °C for 02 h to remove the carboxymethylcellulose.

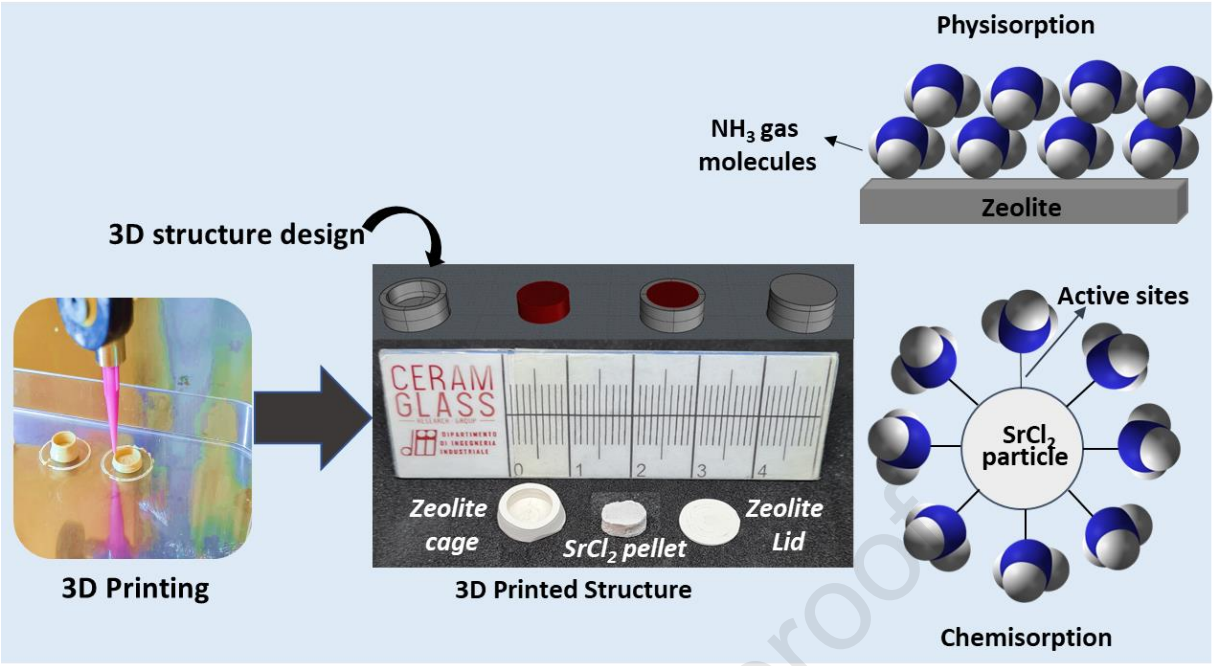

Fig. 1: Photo of the 3D printing process, model design of the composite structure, photographs of the 3D printed zeolite cage and $SrCl_2$ pellet, and a schematic of the sorption mechanisms on zeolite and $SrCl_2$.

2.2 NH_3 sorption experiments:

The NH_3 sorption measurements were performed on a High IsoSORP sorption apparatus (High-pressure TGA, TA instrument, New Castle, DE, USA). The device comprises a magnetic suspension balance, an electrical heater, a vacuum pump, and an oil bath. A certain amount of sample was loaded into the measuring chamber. The specimens were first degassed under evacuation at 150 ^oC for 03 h. After that, buoyancy measurement was performed using helium (purity 99.99%) to evaluate the mass and volume of the sample at 10 bar pressure and 20 ^oC. The system was purged 5 times before buoyancy measurement to ensure no residual adsorbate gas (NH_3) from the previous experiments. Next, the gas was switched from He to NH_3 with a setpoint pressure of 3 bar and 20 ^oC. Again, the system was purged 5 times before starting the experiment to ensure the gas pipeline has pure NH_3 gas. Finally, the sorption experiment was carried out at 3 bar and desorption at 0 bar (vacuum). All the experiments were carried out under the same conditions, and 10 cycles were performed for the $SrCl_2$ pellet inside the zeolite cage (SPZC). Thermal regeneration was done between the cycles, and the buoyancy test was measured separately.

2.3 Characterizations of sorbents:

3D printed structures were characterised characterized using various analytical techniques. The microstructure of the material was investigated using a scanning electron microscope (Magellan 400 Extreme-High Resolution SEM, FEI Company, Eindhoven, Netherlands). Crystal structure and diffraction patterns were collected from the components ground into fine powders using CuKα radiation on an X-ray diffractometer (D8 Advance, Bruker Corporation, Germany) with a 0.02° step size and a 1.2 °/min scan speed. The thermal stability of materials was analyzed using thermogravimetric analysis coupled with dynamic scanning calorimetry (TGA/DSC, NETSCH F690) up to 1000 ºC using a heating rate of 10 K/min. Specific Surface Area was measured with an automated gas adsorption analyzer (Autosorb iQ, Anton Paar, Austria) using Ar at 87 K, as recommended by IUPAC guidelines for microporous materials [22]. Samples were degassed at 350 °C under a high vacuum for 08 h before analysis. The linear range for BET SSA calculation was selected at a relative pressure of 0.008-0.04 according to Rouquerol's correction for microporous materials.

3 Results and Discussion:

Evaluating microstructural changes in the structured sorbent allows us to estimate the capacity and stability for NH_3 sorption. The microstructure of $SrCl_2$ salt and zeolite cage was analyzed before and after NH_3 sorption measurements, as shown in Fig. 2. The $SrCl_2$ showed the changes in microstructure. It has developed a porous structure after sorption measurement due to NH_3 gas desorption. Other studies have also reported induced porosity leading to an increase in the surface area of $SrCl_2$ [12]. In Fig. 2c, the $SrCl_2$ pellet confirms the presence of polyethylene glycol (PEG), interconnecting the $SrCl_2$ particles. The $SrCl_2$ pellet also develops a porous structure after NH_3 adsorption and desorption, as shown in Fig. 2d. After desorption, the $SrCl_2$ pellet still demonstrates the interconnectivity of the salt particles owing to the presence of PEG as a binder. None of the images shows the melting spread problem of $SrCl_2$, which suggests that the structure is thermally stable during the NH_3 sorption measurements. Fig. 2(e and f) displays the microstructure of the zeolite cage before and after NH_3 sorption. The 13X crystals and geopolymer flakes can be seen without any change before and after cyclic sorption measurements.

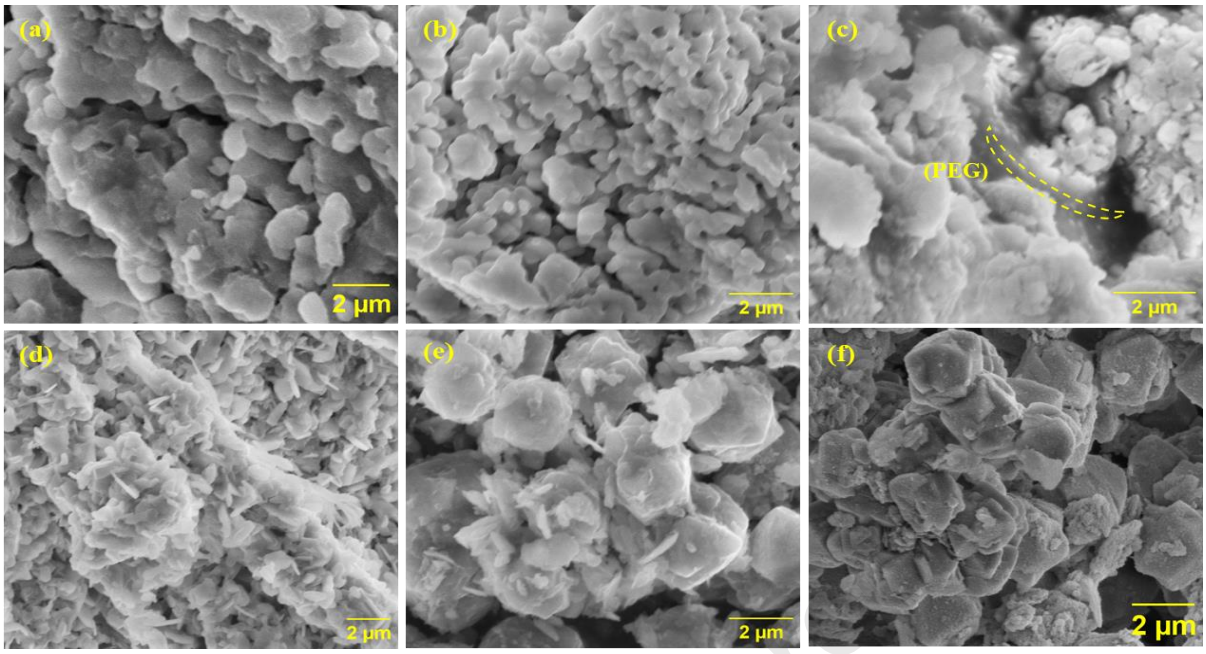

Fig. 2 SEM micrographs of the sorbents; (a) $SrCl_2$, (b) $SrCl_2$ after NH_3 sorption, (c) $SrCl_2$ pellet. (d) $SrCl_2$ pellet after NH_3 sorption, (e) Zeolite cage (f) Zeolite cage after NH_3 sorption.

The X-ray diffractogram of the zeolite-geopolymer cage (Fig. 3) displays all the reflections associated with the initial 13X powder, indicating excellent stability of the zeolite in the geopolymer slurry. Additional peaks were identified as Na-bentonite, which was employed as a rheological additive. Furthermore, the X-ray diffractogram highlights the presence of the geopolymer matrix in the form of a subtle amorphous halo centered around 27° together with a few diffractions associated with crystalline impurities (muscovite, anatase, and quartz) in the metakaolin, which does not take part in the geopolymerisation reaction. The $SrCl_2$ powder was treated at 150 °C before NH_3 sorption tests to simulate the activation process. Anhydrous $SrCl_2$ was identified as the primary phase from the X-ray diffractograms (Fig. 2b), with the dihydrate and hexahydrate forms as minor constituents. A few unidentified peaks are most likely associated with the monohydrate form of $SrCl_2$.

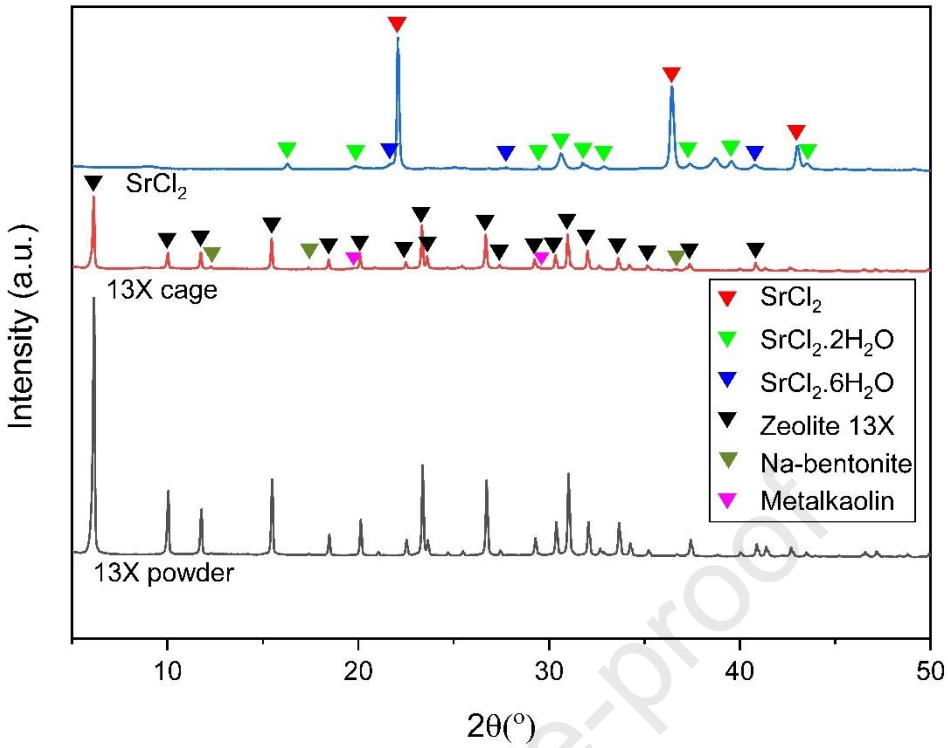

Fig. 3 X-ray diffractograms of zeolite 13X powder, 3D printed 13X-geopolymer composite cage, and $SrCl_2$ after activation at 150 °C.

Fig. 4 shows the adsorption isotherms to evaluate the surface area and pore structure. As shown in Fig. 4a, both the initial 13X powder and the 13X-geopolymer composites display a Type I isotherm characterized by a high uptake of adsorbate at low pressure, indicating micropores. However, the composite also reveals the presence of some degree of macroporosity, as evidenced by the uptick of the isotherm as it approaches saturation. For the initial zeolite 13X powder, the SSA was 708 $m^2g^{-1,}$ and a pore volume of 0.308 cm^3g^{-1} were measured, consistent with the data reported in the literature [23]. The values for the 13X-geopolymer composite cage were calculated as 366 m^2g^{-1} and 0.216 cm^3g^{-1} for SSA and pore volume, respectively. The SSA value is slightly lower than the theoretical value of the composite, assuming 60 wt.% zeolites, which are completely accessible to the adsorbate. The data may indicate a partial occlusion of the zeolites by the geopolymer matrix or by residual CMC, which was not entirely removed by heat treatment. The pore volume is higher than expected for the composite owing to the intrinsic macroporosity of the geopolymer matrix.

The isotherm for bentonite was measured using N_2 at 77K, yielding a BET SSA value of 54 m^2g^{-1} (P/P_0 range of 0.03-0.15) and a pore volume of 0.123 cm^3g^{-1}. As shown in Fig. 4b, the

isotherm can be ascribed to a Type IV with a Type H3 hysteresis loop, indicating the presence of mesopores with a slit-shaped morphology. The shape of the isotherm at low P/P_0 values suggests that a small fraction of large micropores may also be present [24][25][26]. No influence of bentonite on the textural properties of the composite could be detected, likely because of the small volume fraction used in the formulation. The $SrCl_2$ powder, measured with N_2 at 77 K, yielded an SSA of 1 m^2g^{-1}, indicating the essentially non-porous nature of the material [12].

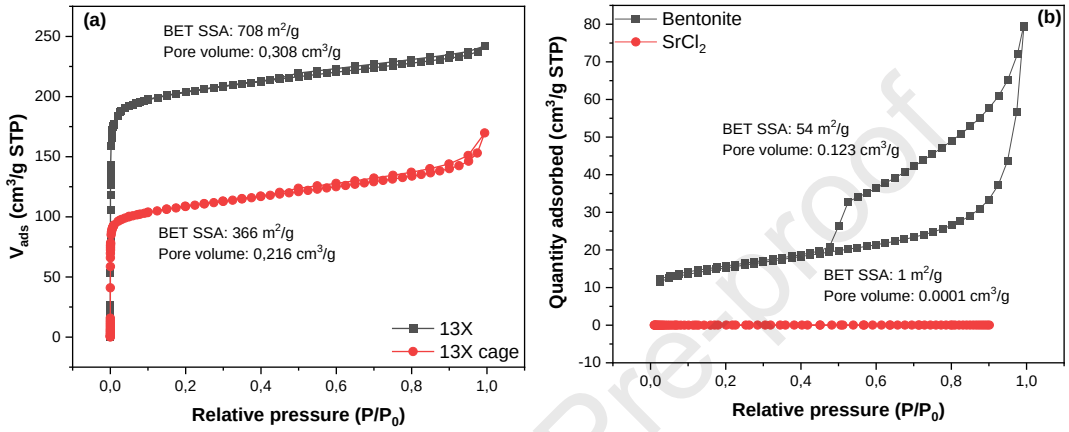

Fig. 4 Argon adsorption-desorption isotherms for the zeolite 13X powder and 3D printed 13X-geopolymer composite cage measured at 87 K (a), and nitrogen adsorption-desorption isotherms for Na-bentonite and $SrCl_2$ measured at 77 K (b).

The thermal stability of the crystal structures of zeolite and $SrCl_2$ was evaluated through TGA-DSC analysis, as shown in Fig. 5 (a and b). All of the samples displayed good stability. The $SrCl_2$ showed two small peaks, visible in the DSC plot below 200 ^oC corresponding to stepwise dehydration and removal of free moisture [27][28]. There is a peak at 875 ^oC which shows the melting of $SrCl_2$. The melting spread has been reported as a problem in the NH_3 sorption process owing to the high exothermic heat of the amine complex formation. The $SrCl_2$ pellet shows more significant peaks around 130 ^oC, which could be the melting of PEG-2000 and the dehydration of $SrCl_2$. The 13X showed moisture removal below 200 ^oC and an exothermic peak at 907 ^oC possibly due to phase transformation [29]. At high temperatures, typically above 800 C, the crystalline 13X zeolite transforms into an amorphous aluminosilicate, and the amorphous phase recrystallizes into a nepheline phase by releasing the energy with the temperature increase [30][31][32]. The bentonite showed two peaks apart from free moisture loss below 200 ^oC. The peak at 632 ^oC represents the loss of lattice water, and a second peak at 857 ^oC corresponds to the presence of a small quantity of montmorillonite and illite in bentonite clay [33]. As per

TGA/DSC results, all the components of SPZC structure are stable till 800 °C, therefore, thermal treatment of the structure (at 450 °C as mentioned in methodology section) would not affect the crystallinity of the materials.

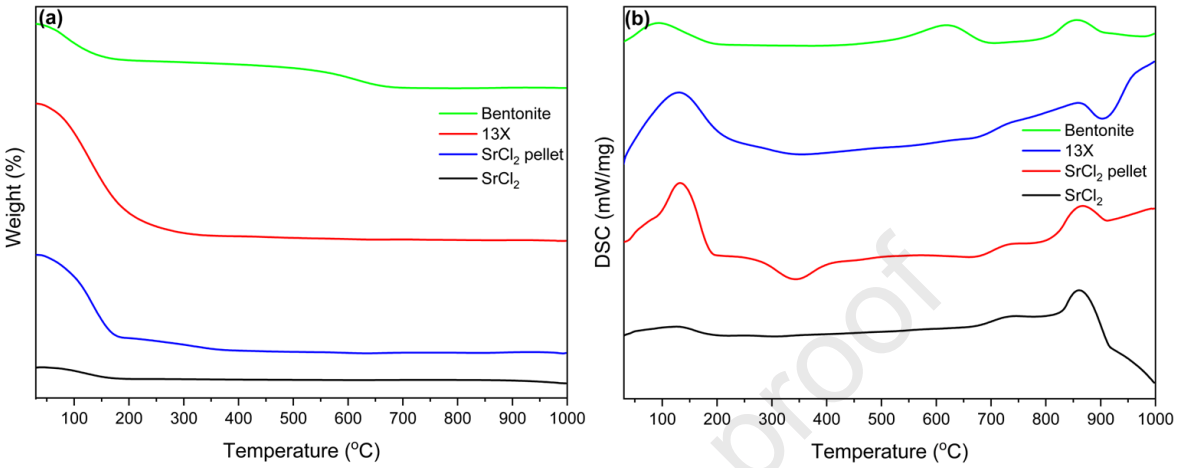

Fig.5 (a) Thermogravimetric (TGA) plots (b) Differential scanning calorimetry (DSC) plots of bentonite, zeolite 13X, $SrCl_2$ powder, and pellet.

Fig. 6(a) shows the screening experiments showing the performance of various components of the designed structure. The sourced $SrCl_2$ powder exhibited the highest NH_3 sorption capacity of 842 mg/g. The structured $SrCl_2$ pellet showed the maximum NH_3 uptake of 820 mg/g, corresponding to the mass composition of $SrCl_2$ in the pellet. The $SrCl_2$ involves adsorption of the NH_3 through the chemisorption process, which proceeds through the formation of a metal-amine complex as shown in equation (1):

$$SrCl_2 + 8NH_3 \leftrightarrow Sr(NH_3)_8Cl_2 \quad (1)$$

where 8 molecules of NH_3 are bonded to the $SrCl_2$. The empty zeolite cage showed an NH_3 uptake of 43 mg/g, which is low compared to the $SrCl_2$. The zeolites capture the NH_3 employing van der Waals force (dipole moment of NH_3 molecules) and electrostatic attraction of exchangeable cations that attach the gas molecules with adsorbent particles [32]. For the SPZC, the sorption capacity is higher than zeolite but lower than the pellet. The sorption capacity is calculated by measuring the amount of solute (NH_3) adsorb per gram of the adsorbent. In SPZC, the weight of the pellet is low compared to the zeolite cage. Therefore, a high NH_3 capacity of the pellet is shadowed by calculating the capacity per gram. In the SPZC structure concept, a

calculated free space exists inside the cage, so the overall structure remains intact during sorption. The $SrCl_2$ expands three times during the adsorption of NH_3, so the SPZC structure can accommodate the volume changes without losing the overall structural integrity and capacity. In addition, an exothermic metal-amine formation reaction generates heat which on accumulation can cause sintering or melting of the sorbent. In the SPZC composite structure, the 3D printed zeolite cage was found stable before and after ammonia sorption, and it showed the characteristic crystals of 13X zeolite, Fig. 2 e, and f, suggesting the structural stability and potential of utilization of SPZC for various purposes.

Pressure is an important parameter in a gas adsorption system. Fig. 6(b) shows the effect of pressure on the NH_3 uptake of different adsorbents. Equilibrium pressure (p) for $SrCl_2$ at reaction temperature can be estimated using Van't Hoff equation as shown below:

$$\ln(p) = -\frac{\Delta H}{RT} + \frac{\Delta S}{R} \quad (2)$$

where T is the temperature, R is the universal gas constant, ΔH is the enthalpy of adsorption, and ΔS is the entropy. Reported values of ΔH and ΔS are 41.4 $kJ.mol^{-1}$ and 228.8 $J.mol^{-1}.K^{-1}$, respectively [34]. Using equation (2), value of equilibrium pressure for $SrCl_2$ at 20 ^oC is 0.4 bar. The $SrCl_2$ pellet doesn't show any NH_3 uptake below 0.4 bar pressure, which could be a drawback for low-pressure applications. The capacity of adsorbents increases with pressure, and for the $SrCl_2$ pellet, sorption increases exponentially at higher pressure values. Equation (1) shows the decrease in moles from reactants to the product. Therefore, an increase in pressure will lead to the coordination of more NH_3 molecules to cations of metal halides and a higher rate of metal-amine complex formation. For the zeolite cage, adsorption dominates at the low-pressure region, and 65% of NH_3 adsorption occurs below 0.2 bar. It increases with an increase in pressure, but the effect of the rise in pressure is not so significant after 0.6 bar. The highly microporous adsorbents are characterized by physisorption in at low pressure due to Van der Waals forces and electrostatic attraction [35][18].The SPZC structure shows adsorption at low and high pressure [36] owing to the synergistic effect of the sorption properties of zeolites and AEMHs. The curve at low pressure is analogous to that of the zeolite curve [37][38][39]. Thus, the SPZC demonstrated the potential to be used for NH_3 sorption for applications from low and high-pressure.

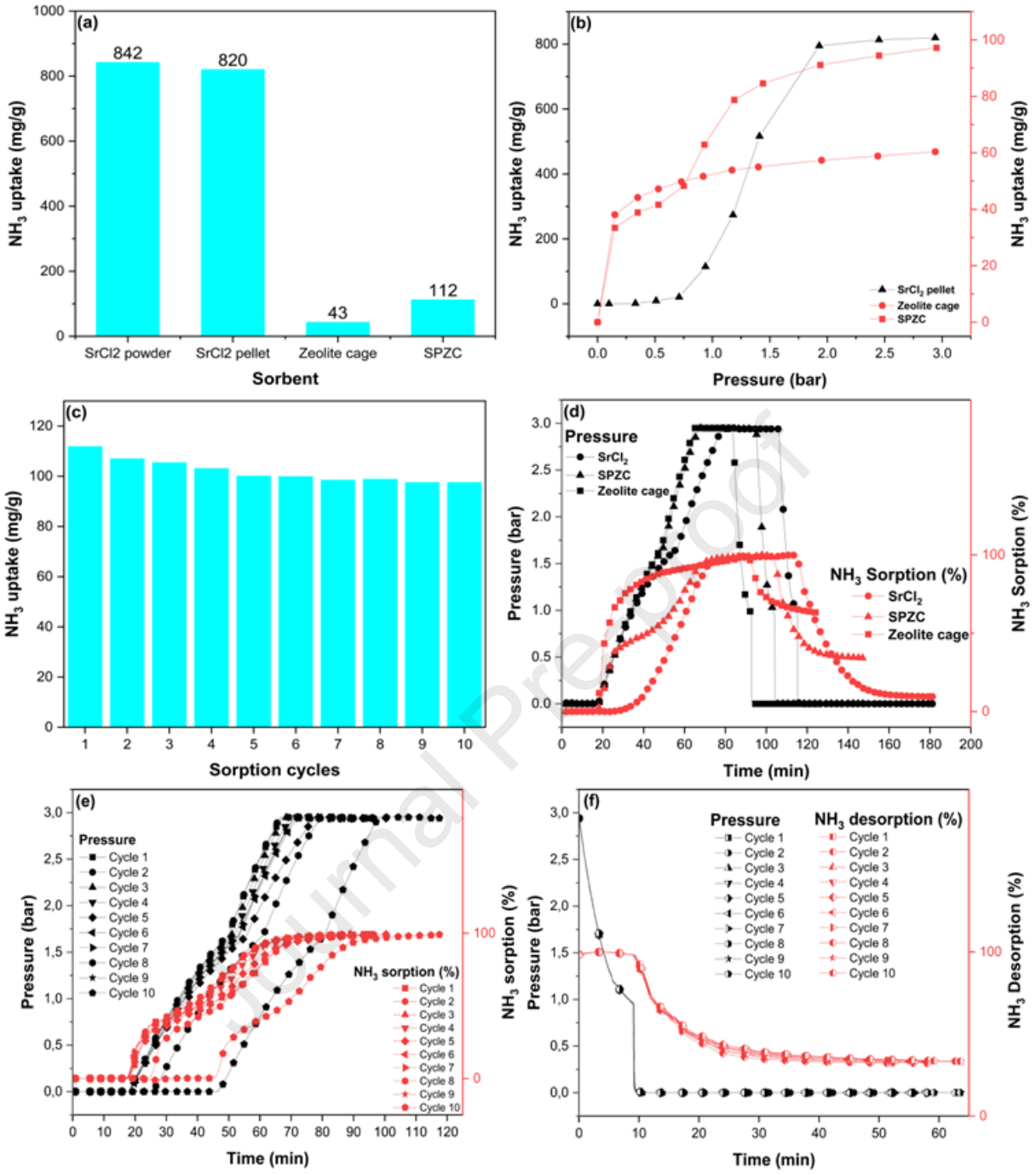

Fig. 6 (a) The NH_3 uptake capacity of $SrCl_2$ powder, $SrCl_2$ pellet, zeolite cage, and SPZC structure at 20 ^oC and 3 bar. (b) Effect of pressure on NH_3 sorption capacity of the $SrCl_2$ pellet, zeolite cage, and SPZC structure. (c) Cyclic NH_3 sorption measurements for SPZC structure. (d) NH_3 sorption kinetics plots of adsorption, desorption, and pressure for $SrCl_2$ powder, zeolite cage, and SPZC structure at 20 ^oC. (e) The pressure curves and NH_3 sorption % of SPZC structure, for 10 cyles of NH_3 sorption from vacuum to 3 bar at 20 ^oC. (f) The pressure curves and NH_3 sorption % of SPZC structure for 10 cylcles of NH_3 desorption from 3 bar to vacuum at 20 ^oC.

Fig. 6(c) shows the cyclic adsorption capacity of the SPZC structure for 10 consecutive cycles. During the cyclic measurements, the sample was regenerated, followed by buoyancy measurements and NH_3 sorption under the same conditions. However, buoyancy was not needed for the cycles when the chamber was kept closed. As shown in Table 1, there is almost no change in the sorption capacity of the structure. Nevertheless, a little decrease can be seen between the first few cycles, which could be due to melting and recrystallization of the PEG binder during cyclic measurement leading to surface coverage of the $SrCl_2$ particles and absorbed ammonia on zeolites which cannot be recovered only with the application of evacuation conditions. A slight decrease (6.3%) in NH_3 sorption of $SrCl_2$ has also been reported by Brynjarsson et al. due to salt's repeated thermal expansion (1300 cycles), which created separate particles from the bed in the thermal energy storage system [41]. However, Cao et al. have reported an unchanged sorption capacity of $SrCl_2$ composites for cyclic experiments [12]. The cyclic experiments show that the SPZC structure can be regenerated and used to > 90% of the sorption capacity for industrial applications without needing replacement.

Table 1 Cyclic performance of SPZC structure for NH_3 sorption and desorption

Sorption cycles	NH_3 uptake (mg/g)	Sorption time (min)	Desorption time (min)
1	112	77	52
2	107	71	52
3	106	71	52
4	103	71	57
5	100	82	58
6	100	77	57
7	98	71	58
8	99	71	57
9	98	71	63
10	98	71	64

In the SCR system, NH_3 is injected into the engine exhaust gases, and then the mixture passes over a catalyst where NOx emissions are transformed into N_2 and H_2O. The continuous supply of the reductant is essential, therefore, the rate of NH_3 charging (adsorption) and discharging (desorption) cycle is very important. Therefore, faster sorption kinetics are highly desired characteristics of sorbent. The kinetic sorption data showing an increase in pressure and percent

NH_3 adsorption for different materials is plotted in Fig. 6(d,e) for different materials and cyclic adsorption data for SPZC structure. For the $SrCl_2$ powder, the sample showed no uptake of NH_3 below 0.4 bar which is also supported by van't hoff plot that the equilibrium pressure for $SrCl_2$ powder at 20 ^oC is 0.4 bar. Meanwhile, $SrCl_2$ exhibited an increased uptake with pressure and reached saturation in 81 min. It shows the sluggish kinetics of NH_3 adsorption of AEMHs. The zeolite cage shows a steep increase in capacity at lower pressure below 0.4 bar, which continues to increase until the material reaches saturation capacity. The steep curve shows the adsorption of NH_3, where molecules quickly find the sites over a high surface area microporous zeolite 13X sorbent [6][42]. The zeolite13X reached 80% of the saturation capacity in 35 min, whereas $SrCl_2$ reached the same saturation level in 65 min owing to fast sorption kinetics for the physisorption process. In the SPZC structure, both components contribute differently according to the sorption mechanisms. The SPZC took 61 min to reach 80% of the saturation capacity, less than powder samples and longer than zeolite. The SPZC structure exhibited two different sorption mechanisms; (1) physisorption and (2) chemisorption. The sharp increase in NH_3 uptake at the low-pressure region is due to physical adsorption by zeolite. On the other hand, the NH_3 uptake continues to slowly increase at high-pressure regions owing to dominant chemisorption by $SrCl_2$. The synergistic effect of physical and chemical sorption contributed to the improved kinetics, an additional advantage of adopting the current approach. Besides, volume expansion is completely accommodated in the logical design of SPZC structure.

The adsorption mechanism of NH_3 molecules involves the adsorption on the surface, overcoming the surface mass transfer resistance and diffusing into bulk sites immediately below the surface and then further diffusion into the bulk of material [39]. Therefore, the diffusivity of each sorbent was estimated using the following equation (3):

$$1 - \theta \approx \frac{6}{\pi^2} \exp\left(-\frac{\pi^2 D t}{r^2}\right) \qquad (3)$$

where θ is the fractional adsorption (ratio of adsorption of solute at any time t to the maximum adsorption at equilibrium), r is the radius of the adsorbent's crystal, and D is the diffusivity. The diffusivity for $SrCl_2$, SPZC, and zeolite cage was estimated using the reported method [35] [12]. The calculated values of diffusion time constant are 9.15×10^{-5}, 6.79×10^{-4}, and 5.99×10^{-4} s^{-1} for $SrCl_2$, SPZC, and zeolite cage, respectively. The data shows higher mass transfer kinetics of SPZC structure compared to $SrCl_2$ powder. The zeolite having a porous structure showed the highest diffusion time constant value, thereby quickly reaching saturation capacity. However, the drawback of this approach is the limitation of data fitting in specific pressure

regions. The mass transfer coefficient of $SrCl_2$ was estimated for an adsorption capacity of < 5%, whereas zeolite model fitting was performed for adsorption greater than 70% [12][34][43].

Desorption kinetics in Fig. 6(d, f) shows desorption took place with a decrease in pressure without applying heat for different materials and cyclic data for SPZC structure. The NH_3 molecules from the $SrCl_2.8NH_3$ complex were desorbed to $SrCl_2.NH_3$, by removing the pressure to vacuum conditions, which shows the salt's practicality for easy regeneration. The sample can be reused without undergoing any changes in structure. In addition, monoamine $SrCl_2.NH_3$ has been reported as a stable phase at STP and needs thermal treatment for regeneration back to $SrCl_2$ [44]. The NH_3 molecules attached to the $SrCl_2$ has different bond length, the monoamine has shorter bond length than octa-amine; therefore, a high amount of energy is needed to remove the monoamine from $SrCl_2$ [39]. The time required to regenerate $SrCl_2$ powder was 76 min. Meanwhile, the zeolite cage and SPZC structure were regenerated in 42 and 54 min, respectively. The desorption time for $SrCl_2$ was longer than the zeolite cage and SPZC structure which may be due to sluggish kinetics owing to chemisorbed NH_3 molecules. Considering the working capacity without thermal treatment, $SrCl_2$ can readsorb 7 molecules of NH_3, approximately 87% of the saturation capacity at given pressure conditions. Therefore, thermal regeneration can be completely avoided, and time for regeneration could be decreased, which is necessary for commercial applications. Vacuum regeneration has also been reported by Liu et al. where it was observed that evacuation cannot fully regenerate the sorbent [38]. Similarly, Kubota et al. reported that desorption for the metal ammine complex depends on the temperature and concentration of NH_3 [45]. This study demonstrated that removing NH_3 concentration, i.e., applying a vacuum, could be a more efficient way to regenerate the adsorbent. Overall, the rational design of SPZC structures demonstrates the potential for commercial application in the SCR system and H_2 carrier in the form of NH_3.

4 Conclusion

In summary, we have shown that a rationally designed 3D-printed novel SPZC structure can effectively overcome the volume expansion challenge in the NH_3 storage over AEMHs. The novel structure showed stable sorption performance for numerous cycles without changing the microstructure, as analyzed by the SEM. The synergistic effect of physicochemical adsorption owing to the $SrCl_2$ and zeolite enabled the better performance of the SPZC structure at different pressure with improved sorption and mass transfer kinetics. Further, applying evacuation conditionsavoided the thermal energy needed for regeneration. The sorbent recovered and reached 87.5% of the working capacity after vacuum regeneration, rendering the process

economical and efficient. Hence, rationally designed AEMHs-based NH_3 sorbents unit can potentially replace the urea solution in the SCR system and ensure the smooth injection of NH_3 into SCR reaction chamber at different ambient conditions leading to efficient NOx reduction.

Acknowledgment:

The research was funded by Formas grant no. 2016-01099 and VR grant no. 2018-04407. The authors acknowledge Dr. Zhejian Cao for training and guidance on high-pressure TGA equipment. The authors acknowledge Lars Frisk for his support of safety in the NH_3 sorption facility.

Author contribution statement:

Nasir Shezad; Marco D'Agostini; Ali Ezzine: Performed the experiments; Analyzed and interpreted the data; Wrote the paper. Giorgia Franchin; Paolo Colombo; Farid Akhtar: Conceived and designed the experiments; Analyzed and interpreted the data; Contributed reagents, materials, analysis tools or data; Wrote the paper.

Data availability statement:

Data will be made available on request.

Conflict of Interest:

The authors declare no conflict of interest.

References:

[1] Y. Ogen, "Assessing nitrogen dioxide (NO_2) levels as a contributing factor to coronavirus (COVID-19) fatality," *Sci. Total Environ.*, vol. 726, no. March, p. 138605, 2020, doi: 10.1016/j.scitotenv.2020.138605.

[2] X. Wu, R. C. Nethery, M. B. Sabath, D. Braun, and F. Dominici, "Air pollution and COVID-19 mortality in the United States: Strengths and limitations of an ecological regression analysis," *Sci. Adv.*, vol. 6, no. 45, pp. 1–7, 2020, doi: 10.1126/SCIADV.ABD4049.

[3] J. H. Baik *et al.*, "Control of NOx emissions from diesel engine by selective catalytic reduction (SCR) with urea," *Top. Catal.*, vol. 30–31, no. x, pp. 37–42, 2004, doi: 10.1023/b:toca.0000029725.88068.97.

[4] Y. Liu, J. Zhao, and J. M. Lee, "Conventional and New Materials for Selective Catalytic

Reduction (SCR) of NOx," *ChemCatChem*, vol. 10, no. 7, pp. 1499–1511, 2018, doi: 10.1002/cctc.201701414.

[5] P. Tan, X. Li, S. Wang, Z. Hu, and D. Lou, "Selective catalytic reduction failure of low NH_3-NOx ratio," *Chinese J. Chem. Eng.*, vol. 32, pp. 231–240, 2021, doi: 10.1016/j.cjche.2020.07.055.

[6] C. J. Doonan, D. J. Tranchemontagne, T. G. Glover, J. R. Hunt, and O. M. Yaghi, "Exceptional ammonia uptake by a covalent organic framework," *Nat. Chem.*, vol. 2, no. 3, pp. 235–238, 2010, doi: 10.1038/nchem.548.

[7] T. D. Elmøe, R. Z. Sørensen, U. Quaade, C. H. Christensen, J. K. Nørskov, and T. Johannessen, "A high-density ammonia storage/delivery system based on $Mg(NH_3)_6Cl_2$ for SCR-DeNOx in vehicles," *Chem. Eng. Sci.*, vol. 61, no. 8, pp. 2618–2625, 2006, doi: 10.1016/j.ces.2005.11.038.

[8] G. Fulks, G. B. Fisher, K. Rahmoeller, M. C. Wu, E. D'Herde, and J. Tan, "A review of solid materials as alternative ammonia sources for lean NOx reduction with SCR," *SAE Tech. Pap.*, 2009, doi: 10.4271/2009-01-0907.

[9] R. Z. Sørensen *et al.*, "Indirect, reversible high-density hydrogen storage in compact metal ammine salts," *J. Am. Chem. Soc.*, vol. 130, no. 27, pp. 8660–8668, 2008, doi: 10.1021/ja076762c.

[10] C. H. Christensen *et al.*, "Metal ammine complexes for hydrogen storage," *J. Mater. Chem.*, vol. 15, no. 38, pp. 4106–4108, 2005, doi: 10.1039/b511589b.

[11] P. Berdiyeva, A. Karabanova, D. Blanchard, B. C. Hauback, and S. Deledda, "$Sr(NH_3)_8Cl_2$-Expanded Natural Graphite composite for thermochemical heat storage applications studied by in-situ neutron imaging," *J. Energy Storage*, vol. 34, p. 102176, 2021, doi: 10.1016/j.est.2020.102176.

[12] Z. Cao and F. Akhtar, "Porous Strontium Chloride Scaffolded by Graphene Networks as Ammonia Carriers," *Adv. Funct. Mater.*, vol. 31, no. 30, 2021, doi: 10.1002/adfm.202008505.

[13] Z. Cao, *Structured Ammonia Carriers for Selective Catalytic Reduction*. 2021.

[14] Z. Cao, N. Grimaldos Osorio, X. Cai, P. Feng, and F. Akhtar, "Carbon-reinforced $MgCl_2$ composites with high structural stability as robust ammonia carriers for selective

catalytic reduction system," *J. Environ. Chem. Eng.*, vol. 8, no. 1, p. 103584, 2020, doi: 10.1016/j.jece.2019.103584.

[15] F. Cao, Zhejian; Narang, Kritika; Akhtar, "Rapid Ammonia Carriers for SCR Systems Using," vol. 2, 2020.

[16] "Pros and cons with Freeze graulation vs Spray Drying." https://powderpro.se/background/pros-cons/ (accessed Jul. 02, 2022).

[17] B. Yeskendir, J. Dacquin, Y. Lorgouilloux, and C. Courtois, "Materials Advances From metal – organic framework powders to shaped solids : recent developments and challenges," pp. 7139–7186, 2021, doi: 10.1039/d1ma00630d.

[18] C. Y. Liu and K. ichi Aika, "Ammonia Adsorption on Ion Exchanged Y-zeolites as Ammonia Storage Material," *J. Japan Pet. Inst.*, vol. 46, no. 5, pp. 301–307, 2003, doi: 10.1627/jpi.46.301.

[19] M. P. Bernal and J. M. Lopez-Real, "Natural zeolites and sepiolite as ammonium and ammonia adsorbent materials," *Bioresour. Technol.*, vol. 43, no. 1, pp. 27–33, 1993, doi: 10.1016/0960-8524(93)90078-P.

[20] M. R. Adam *et al.*, "Influence of the natural zeolite particle size toward the ammonia adsorption activity in ceramic hollow fiber membrane," *Membranes (Basel).*, vol. 10, no. 4, pp. 1–18, 2020, doi: 10.3390/membranes10040063.

[21] M. Yamaguchi, T. Ichikawa, H. Miyaoka, T. Zhang, H. Miyaoka, and Y. Kojima, "Proton-based solid acids for ammonia absorption in ammonia water," *Int. J. Hydrogen Energy*, vol. 45, no. 41, pp. 22189–22194, 2020, doi: 10.1016/j.ijhydene.2020.05.255.

[22] M. Thommes *et al.*, "Physisorption of gases, with special reference to the evaluation of surface area and pore size distribution (IUPAC Technical Report)," *Pure Appl. Chem.*, vol. 87, no. 9–10, pp. 1051–1069, 2015, doi: 10.1515/pac-2014-1117.

[23] E. Masika and R. Mokaya, "Preparation of ultrahigh surface area porous carbons templated using zeolite 13X for enhanced hydrogen storage," *Prog. Nat. Sci. Mater. Int.*, vol. 23, no. 3, pp. 308–316, Jun. 2013, doi: 10.1016/J.PNSC.2013.04.007.

[24] L. A. Shah, M. das G. da Silva Valenzuela, M. Farooq, S. A. Khattak, and F. R. Valenzuela Díaz, "Influence of preparation methods on textural properties of purified bentonite," *Appl. Clay Sci.*, vol. 162, pp. 155–164, Sep. 2018, doi:

10.1016/J.CLAY.2018.06.001.

[25] S. Ai, Y. Huang, T. Xie, X. Zhang, and C. Huang, "Fabrication of composites with ultra-low chitosan loadings and the adsorption mechanism for lead ions," *Environ. Sci. Pollut. Res.*, vol. 27, no. 30, pp. 37927–37937, Oct. 2020, doi: 10.1007/S11356-020-09906-7/TABLES/6.

[26] I. F. Macías-Quiroga, A. Pérez-Flórez, J. S. Arcila, G. I. Giraldo-Goméz, and N. R. Sanabria-Gonzalez, "Synthesis and Characterization of Co/Al-PILCs for the Oxidation of an Azo Dye Using the Bicarbonate-Activated Hydrogen Peroxide System," *Catal. Letters*, vol. 152, no. 7, pp. 1905–1916, Sep. 2021, doi: 10.1007/S10562-021-03788-1/FIGURES/8.

[27] M. A. R. Blijlevens *et al.*, "A study of the hydration and dehydration transitions of $SrCl_2$ hydrates for use in heat storage," *Sol. Energy Mater. Sol. Cells*, vol. 242, p. 111770, Aug. 2022, doi: 10.1016/J.SOLMAT.2022.111770.

[28] R. J. Clark and M. Farid, "Experimental investigation into the performance of novel $SrCl_2$-based composite material for thermochemical energy storage," *J. Energy Storage*, vol. 36, p. 102390, Apr. 2021, doi: 10.1016/J.EST.2021.102390.

[29] S. K. Lakhera, H. A. Sree, and S. Suman, "Synthesis and characterization of 13x zeolite/ activated carbon composite," *Int. J. ChemTech Res.*, vol. 7, no. 3, pp. 1364–1368, 2015.

[30] M. K. Król and P. Jeleń, "The effect of heat treatment on the structure of zeolite a," *Materials (Basel).*, vol. 14, no. 16, Aug. 2021, doi: 10.3390/MA14164642/S1.

[31] T. Palenta, S. Fuhrmann, G. N. Greaves, W. Schwieger, and L. Wondraczek, "Thermal collapse and hierarchy of polymorphs in a faujasite-type zeolite and its analogous melt-quenched glass," *J. Chem. Phys.*, vol. 142, no. 8, p. 084503, Feb. 2015, doi: 10.1063/1.4913240.

[32] F. Akhtar and L. Bergström, "Colloidal processing and thermal treatment of binderless hierarchically porous zeolite 13X monoliths for CO_2 capture," *J. Am. Ceram. Soc.*, vol. 94, no. 1, pp. 92–98, 2011, doi: 10.1111/j.1551-2916.2010.04044.x.

[33] M. Sarkar, K. Dana, S. Ghatak, and A. Banerjee, "Polypropylene-clay composite prepared from Indian bentonite," *Bull. Mater. Sci.*, vol. 31, no. 1, pp. 23–28, 2008, doi: 10.1007/s12034-008-0005-5.

[34] A. L. Ammitzboll, S. Lysgaard, A. Klukowska, T. Vegge, and U. J. Quaade, "Surface adsorption in strontium chloride ammines," *J. Chem. Phys.*, vol. 138, no. 16, 2013, doi: 10.1063/1.4800754.

[35] D. Saha and S. Deng, "Ammonia adsorption and its effects on framework stability of MOF-5 and MOF-177," *J. Colloid Interface Sci.*, vol. 348, no. 2, pp. 615–620, 2010, doi: 10.1016/j.jcis.2010.04.078.

[36] Y. Chen, F. Zhang, Y. Wang, C. Yang, J. Yang, and J. Li, "Recyclable ammonia uptake of a MIL series of metal-organic frameworks with high structural stability," *Microporous Mesoporous Mater.*, vol. 258, pp. 170–177, 2018, doi: 10.1016/j.micromeso.2017.09.013.

[37] A. Karabanova, P. Berdiyeva, M. van der Pal, R. E. Johnsen, S. Deledda, and D. Blanchard, "Intrinsic kinetics in local modelling of thermochemical heat storage systems," *Appl. Therm. Eng.*, vol. 192, no. March, p. 116880, 2021, doi: 10.1016/j.applthermaleng.2021.116880.

[38] Y. L. Chun and K. I. Aika, "Ammonia absorption into alkaline earth metal halide mixtures as an ammonia storage material," *Ind. Eng. Chem. Res.*, vol. 43, no. 23, pp. 7484–7491, 2004, doi: 10.1021/ie049874a.

[39] A. L. Ammitzboll, S. Lysgaard, A. Klukowska, T. Vegge, and U. J. Quaade, "Surface adsorption in strontium chloride ammines," *Journal of Chemical Physics*, vol. 138, no. 16. 2013, doi: 10.1063/1.4800754.

[40] M. Malmali, G. Le, J. Hendrickson, J. Prince, A. V. McCormick, and E. L. Cussler, "Better Absorbents for Ammonia Separation," *ACS Sustain. Chem. Eng.*, vol. 6, no. 5, pp. 6536–6546, 2018, doi: 10.1021/acssuschemeng.7b04684.

[41] H. Brynjarsson, "Review and Design Adaptations of a $SrCl_2$-NH_3 bench-scale Thermochemical Heat Storage system," 2021.

[42] A. A. Halim, H. A. Aziz, M. A. M. Johari, and K. S. Ariffin, "Comparison study of ammonia and COD adsorption on zeolite, activated carbon and composite materials in landfill leachate treatment," *Desalination*, vol. 262, no. 1–3, pp. 31–35, 2010, doi: 10.1016/j.desal.2010.05.036.

[43] A. Ojuva, F. Akhtar, A. P. Tomsia, and L. Bergström, "Laminated adsorbents with very

rapid CO_2 uptake by freeze-casting of zeolites," *ACS Appl. Mater. Interfaces*, vol. 5, no. 7, pp. 2669–2676, 2013, doi: 10.1021/am400122r.

[44] S. Lysgaard, A. L. Ammitzbøll, R. E. Johnsen, P. Norby, U. J. Quaade, and T. Vegge, "Resolving the stability and structure of strontium chloride amines from equilibrium pressures, XRD and DFT," *Int. J. Hydrogen Energy*, vol. 37, no. 24, pp. 18927–18936, 2012, doi: 10.1016/j.ijhydene.2012.09.129.

[45] M. Kubota, K. Matsuo, R. Yamanouchi, and H. Matsuda, "Absorption and desorption characteristics of NH_3 with metal chlorides for ammonia storage," *J. Chem. Eng. Japan*, vol. 47, no. 7 SPECIAL ISSUE, pp. 542–548, 2014, doi: 10.1252/jcej.13we294.

Declaration of interests

☒ The authors declare that they have no known competing financial interests or personal relationships that could have appeared to influence the work reported in this paper.

☐The authors declare the following financial interests/personal relationships which may be considered as potential competing interests: